Low Reynolds number instabilities and transitions in bluff body wakes

K Hourigan, M C Thompson, G J Sheard, K Ryan, J S Leontini and S A Johnson

Fluids Laboratory for Aeronautical and Industrial Research (FLAIR), Department of Mechanical Engineering, Monash University 3800, Melbourne, Australia

Email: Kerry.Hourigan@eng.monash.edu.au

Abstract. The circular cylinder has been the generic geometry employed to understand many aspects of flows around bluff bodies, including the transition to a turbulent wake flow. The FLAIR group has been interested in the types and orders of instabilities and transitions for a range of bluff body flows. In this paper, variations of the flow from the generic case of a fixed circular cylinder are considered: contraction to a thin plate whilst preserving elliptical profile; elongation of cylinders with elliptical leading edge and square trailing edge: contraction of tori from large major radius to a sphere; and transverse oscillation of a circular cylinder. For elongated cylinders with streamlined leading edges, the analogs of the instability modes for a circular cylinder become unstable in the reverse order. As well, the analogue of mode B has a significantly increased relative spanwise wavelength and appears to have a different near-wake structure. At the other extreme, for a normal flat plate, the wake first becomes unstable to a non-periodic mode that appears distinct from either of the dominant circular cylinder wake modes. For tori, which have a local geometry approaching a two-dimensional circular cylinder for large aspect ratios, the sequence of transitions with increasing Reynolds number is a strong function of aspect ratio. For intermediate aspect ratios, the first occurring wake instability mode is a subharmonic mode. In the case of transversely oscillating cylinders, it is shown that when the two-dimensional wake is in the 2S configuration, modes A, B and QP are present, similar in nature and symmetry structure to the modes of the same names for a fixed cylinder. However, increasing the amplitude of oscillation sees the critical Reynolds number for mode A increase significantly, to the point where mode B becomes critical before mode A. For higher Reynolds numbers, the two-dimensional wake loses its spatio-temporal symmetry and takes on the P + S configuration. With the onset of this configuration, modes A, B and QP cease to exist. It is shown that two new three-dimensional modes (SL and SS) arise from this base flow. The variety of transition modes and order of transition for these different cases may have implications for the route to wake turbulence for such bodies, distinct from that found for a fixed circular cylinder.

1. Introduction

The canonical geometry for two-dimensional bluff bodies has been the circular cylinder. The generic nature of the circular cylinder was strengthened through the Universal Strouhal number formulated by Roshko [1], whereby the two-dimensional wake structures of different short bluff body shapes could be collapsed with respect to the vortex shedding frequency. He proposed using the velocity, which is related to the base pressure, just outside the shear layer at separation rather than the free stream velocity. The universal Strouhal number was also related to the distance between the free shear layers

as they roll up to form vortices. Confirmation of the universal Strouhal number was made by Griffin [2], who undertook experiments to measure this distance for a large range of bluff body shapes.

In recent decades, much interest has been in the appearance in the wake of circular cylinders of three-dimensional instabilities. Both experimental investigations (e.g., Williamson [3-5]; Wu *et al.* [6]; Brede *et al.* [7]; Bays-Muchmore and Ahmed [8]; Gerrard [9]) and computational predictions (e.g. Thompson *et al.* [10,11]; Barkley and Henderson [12]; Henderson [13]; Mittal and Balachandar [14]; Karniadakis and Triantafyllou [15]) have been undertaken of the transition to first mode A (at approximately Re = 190) and then a further bifurcation to mode B (at Re = 230-240). Some differences in the transition Reynolds number occur, particularly for mode B, depending on whether the analysis is a linear analysis, or direct numerical simulations/experiments in which the base flow is modified due to the saturation of mode A. A quasi-periodic mode (QP) is predicted by linear stability analysis to occur at Re = 377; however, it is usually not observed due to significant modification of the base flow by the saturation of mode B at this stage.

Figure 1 shows the streamwise vorticity structure in the wake for modes A and B, which have naturally occurring wavelengths of approximately 4 and 0.8 cylinder diameters, respectively. The fastest growing wavelengths for each mode can be predicted using a Floquet linear stability analysis. The perturbation spanwise and streamwise vorticity fields for two sample wavelengths in the mode A and mode B regimes are shown in figure 2. In addition to direct numerical simulations, the non-linear development of the three-dimensional modes can also be modelled in detail using the Landau equation (e.g., Henderson [13]; Sheard *et al.* [16]).

The question we address in this paper is whether the transition scenario for a fixed circular cylinder, which has been investigated intensively, is in fact generic or universal for two-dimensional shapes. We also consider the wake transition modes as the shape is varied between the circular cylinder and the generic geometry for three-dimensional bluff bodies, the sphere. The FLAIR group at Monash University has devoted considerable effort investigating the effect of body shape and motion on wake transition. In particular, four broadly representative families of body geometry and flow conditions have been examined, which include previously well-studied generic body shapes as limiting cases. The first set consists of the transition from a circular cylinder to a normal flat plate through elliptical cross-sections of decreasing aspect ratio. The second set consists of elongated cylinders with elliptical-leading edges to prevent flow separation except from the trailing edge. The third set focuses on the transition from a circular cylinder (locally) to a sphere, through axisymmetric tori of decreasing aspect ratio placed with their axes aligned with the flow direction. The fourth and final set consists of circular cylinders under transverse forcing of varying amplitudes. These sequences of body shapes and flow conditions are depicted in figure 3. There is, of course, an infinite variety of geometries possible but the current selection is sufficient to demonstrate that, in fact, the sequence and types of transitions in the wake of a fixed circular cylinder are not universal for bluff bodies.

2. Results and Discussion
The wake transitions of the canonical circular cylinder have been discussed above. Now, we consider variations to the geometry and motion, and determine the consequences for the instabilities and transitions in the wake.

2.1. Varying the shape from circular to elliptical to normal flat plate
Johnson *et al.* [17] examined the two-dimensional wake state for a sequence of elliptical bodies with the circular cylinder and flat plate as limiting cases. We discuss here the wake states that arise.

2.1.1. *Elliptical Cylinder.* Visualisations of the circular cylinder wake made by Taneda [18] showed the decay of the Benard-Kármán wake and the growth of a larger secondary structure in the far wake that appeared to be similar to the original Benard-Kármán vortex street, but with a longer wavelength. Taneda concluded that the secondary vortex street was due to an hydrodynamic instability based on the mean velocity profile. Cimbala *et al.* [19] found that the secondary wake structure did not depend
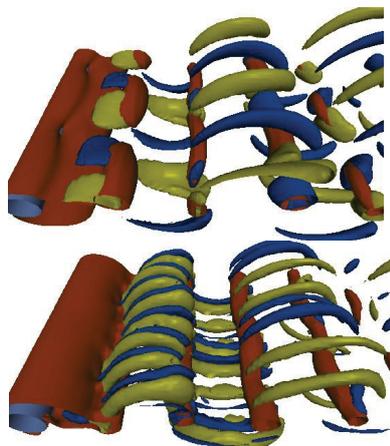
Figure 1. Numerical visualisations of the wake streamwise vorticity for the two shedding modes for a fixed circular cylinder Mode A (Re = 210) is at top and Mode B (Re = 250) is on bottom.
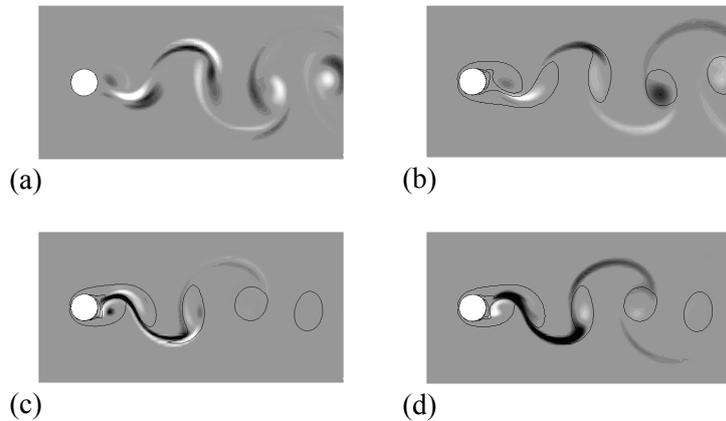

Figure 2. (a) Linear perturbation spanwise and (b) streamwise vorticity for mode A in the wake of a fixed cylinder, Re = 190, λ = 3.0. The mode has just become unstable. (c) Linear perturbation spanwise and (d) streamwise vorticity for mode B in the wake of a fixed cylinder, Re = 260, λ = 0.75. Again, the mode has just become unstable.
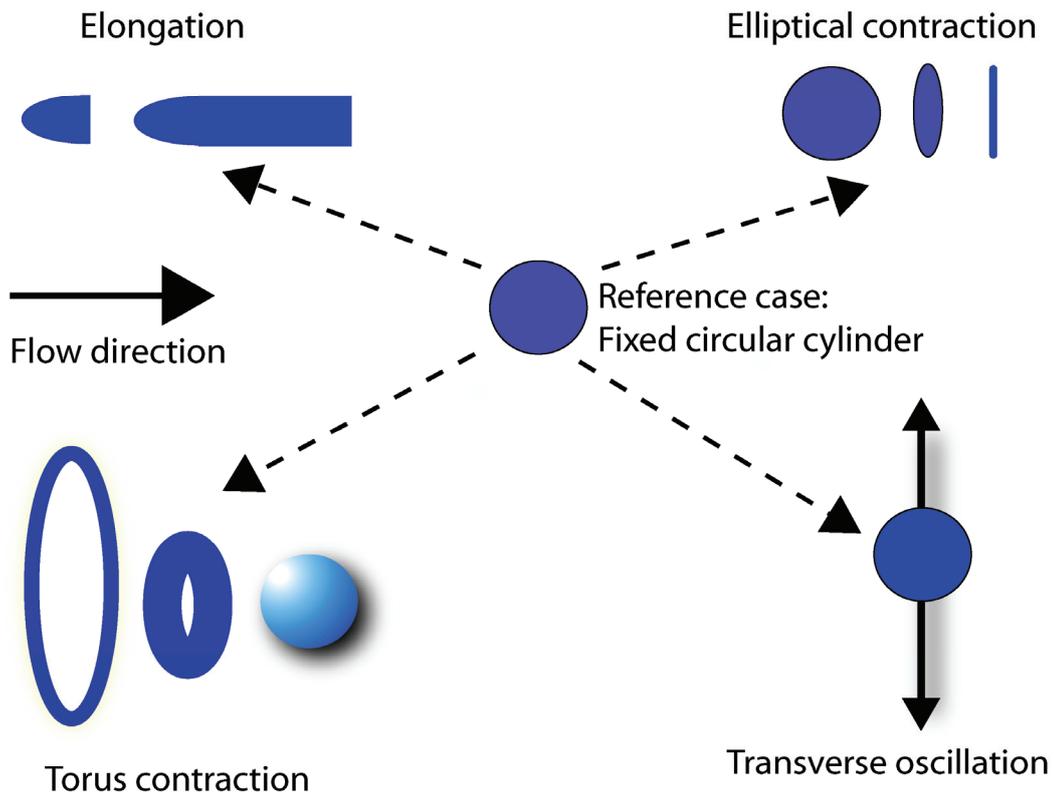

Figure 3 Four variations on the fixed circular cylinder case considered.
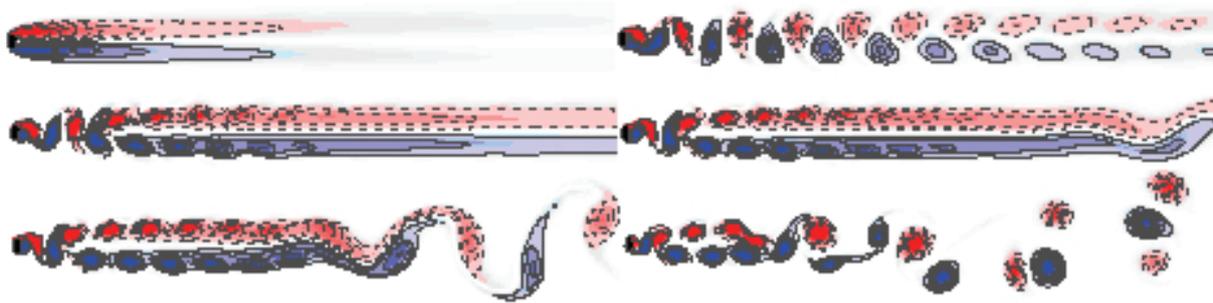
Figure 4. Instantaneous vorticity and streamlines showing wake development for AR=0.5 and Re = 40, 75, 125, 150, 175 and 250 (from left to right, then down). Flow from left to right.

on the scale or frequency of the Benard-Kármán shedding frequency. Rather, their results showed that the frequencies amplified in the far wake were not related to the Benard-Kármán shedding frequency but had good agreement to those found using linear stability theory.

Shown in figure 4 is the development of the wake behind an elliptical cylinder of aspect ratio 0.5 as the Reynolds number is increased: from a steady symmetrical wake (Re = 40), a standard Benard-Kármán street develops and which downstream becomes smeared out into two parallel shear layers (Re = 75); the point of transition to these smeared shear layers moves upstream as Re is increased (Re = 125) and a secondary instability develops within the computed domain downstream (Re = 150); the transition to this secondary instability moves upstream with increasing Reynolds number (Re = 175); eventually other frequencies arise and the wake downstream becomes more chaotic (Re = 250). The effect of increased ellipticity appears to bring upstream the secondary instability that is not found to occur in the fixed circular cylinder wake until perhaps hundreds of diameters downstream [18,19].

2.1.2. *Normal flat plate.* In the limit of ellipticity leading to a normal flat plate, the appearance of the secondary instability occurs at an even lower Reynolds number. At low Reynolds numbers, the wake still resembles the typical Benard-Kármán wake of a circular cylinder (figure 5a). However, by Re = 100 (figure 5b), the secondary instability has moved to the near wake, producing a wake with greater lateral spacing of vortices. Previous studies that have considered this geometry include the three-dimensional numerical simulation of the three-dimensional wake at Re = 250 by Najjar and Balachandar [20] and the investigation of the instability modes for an idealized wake of a normal flat plate by Julien *et al.* [21,22]].

A Floquet stability analysis has been undertaken of this geometry for a range of Reynolds numbers. It was found that, in contrast to the fixed circular cylinder case, the first mode to go unstable was a quasi-periodic mode (having a complex Floquet multiplier) at a Reynolds number of Re = 105–110, with a preferred wavelength of approximately 5–6 plate heights. The second mode to become unstable was a periodic mode of shorter wavelength (2 plate heights) at Re = 125. The Floquet multipliers as a function of spanwise wavelength for these two modes are shown in figure 6 for Re = 130.

Although not the first mode to become unstable and of approximately half the wavelength, the shorter, periodic mode has some similarities to mode A for the fixed circular cylinder. The perturbation streamwise vorticity contours, as well as the position of the spanwise vortex structures, are shown in figure 7 for Re = 130 and wavelengths close to the two fastest growing modes. The spatio-temporal symmetry of the shorter wavelength mode, plus strong evidence of elliptical instability in the vortex cores, is consistent with the classical mode A (Thompson *et al.* [23]).

The longer wavelength instability does not have a period commensurate with the Benard-Kármán shedding frequency; it is a quasi-periodic mode with a complex Floquet multiplier before and after transition. Although this instability is intense in the near wake, it is seen from figure 7b that it decays relatively rapidly downstream. Furthermore, it is found that there is a variability of period with wavelength of this mode, suggesting a rapid breakdown to chaos as the Reynolds number is increased.
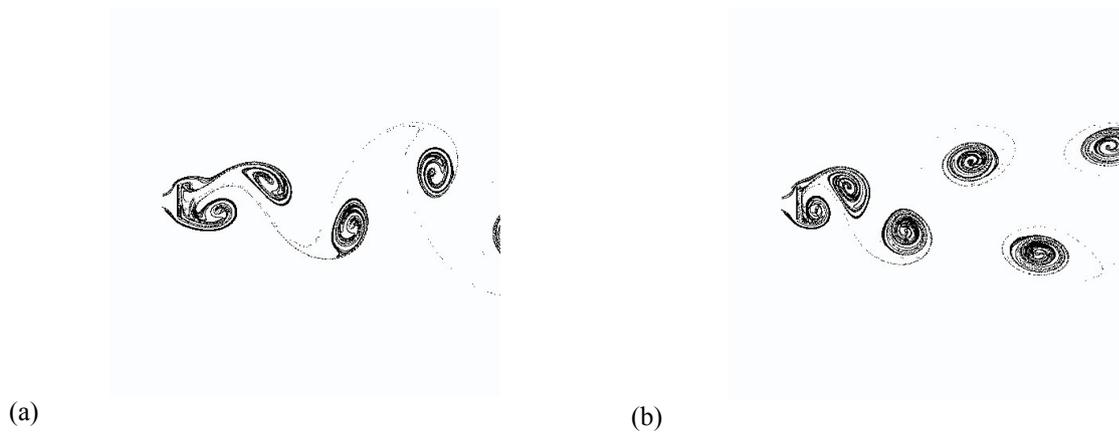
(a)   (b)

Figure 5. Two-dimensional particle traces showing the shedding pattern for flow past a normal flat plate. Flow is from left to right. (a) Re = 40; (b) Re = 100.
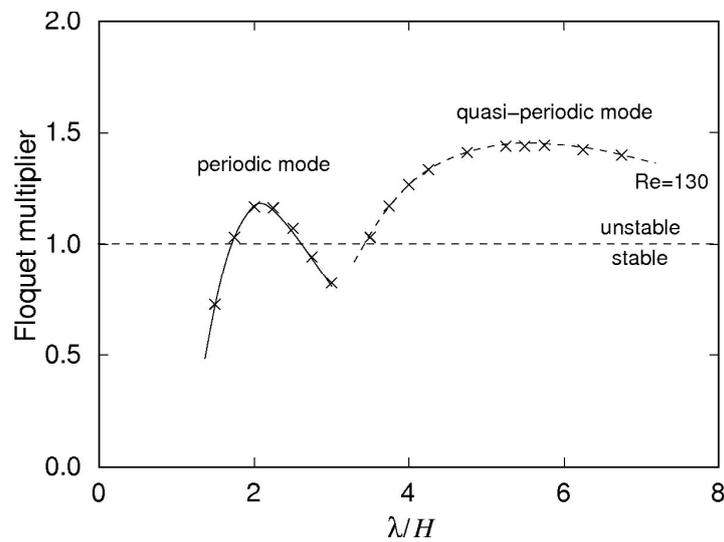

Figure 6. Dominant Floquet multipliers for the wake of a normal flat plate. Re = 130.

(a)   **(b)**   **(c)**
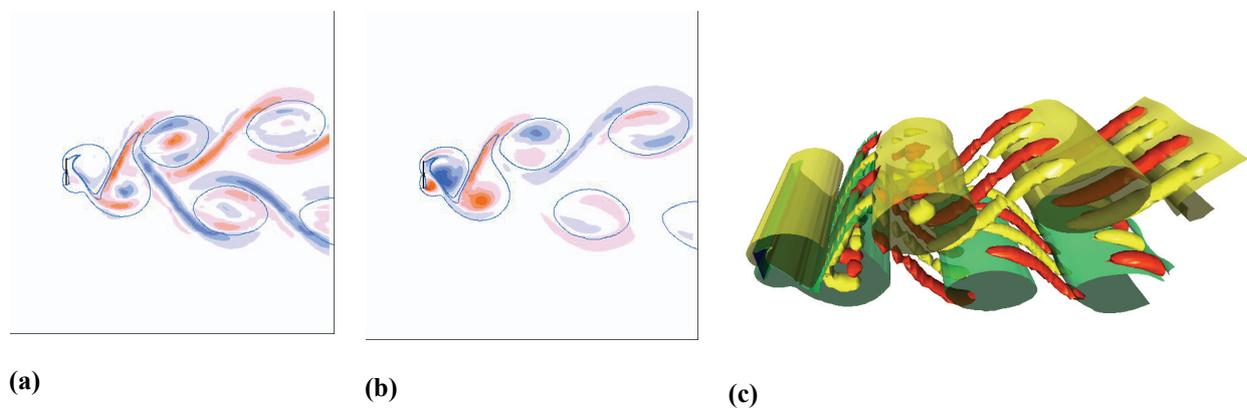
Figure 7. Streamwise perturbation vorticity structure of the first two instability modes for the normal flat plate, Re = 130, for wavelengths of (a) λ/H = 2.25 and (b) λ/H = 5.25, respectively. (c) 3d image of the periodic mode - λ/H = 2.25, showing positions of 2d vortices and the streamwise perturbation vortices. H is the plate height, flow from left to right.

2.2. Varying the shape from circular cylinder to sphere via tori

One of our interests has been to understand the difference in wake transition between a two-dimensional geometry like the circular cylinder and a three-dimensional body like the sphere. This can be achieved by varying the aspect ratio of a torus. When contracted, a sphere results. When expanded, the local flow past a torus asymptotes to that past a circular cylinder. Our studies have included the three-dimensional transitions in the wake (Sheard *et al.* [24]), examination of the saturation of the instability modes using DNS and Landau modelling (Sheard *et al.* [16,25]), and the study of the particular case of transition to a subharmonic mode for a torus of a specific aspect ratio (Sheard *et al.* [26]).

In the current study, we are concentrating on the two-dimensional body but will briefly describe first the wake behaviour for tori of small aspect ratio. Again, emphasis is on the comparison of the type and order of three-dimensional wake modes with the circular cylinder case.

2.2.1. *Small aspect ratio tori.* For aspect ratios below 1.6, the wake flow transitions are similar to those of a sphere. In particular, a regular transition occurs prior to a Hopf bifurcation. Although a dramatic change in topology occurs at AR =1 with the appearance of the central hole, the wake behaviour is continuous across this change. The axisymmetric steady wake undergoes a Hopf bifurcation with azimuthal mode number $m = 1$, in the absence of any regular bifurcation, in the range $1.6 < AR < 1.7$. The regular bifurcation again occurs first at larger aspect ratios, $1.7 \leq AR \leq 3.9$.

2.2.2. *Large aspect ratio tori.* Figure 8 shows the transition Reynolds numbers for the different modes as a function of Reynolds number. Unsurprisingly, in the case where the aspect ratios of the tori were large, three-dimensional modes similar to modes A and B of the circular cylinder wake appeared. Linear stability analysis also predicted a mode C at higher Reynolds number; this mode is not generally observable due to prior saturation of mode B. However, as the aspect ratio is decreased, the Reynolds number for transition to mode C falls dramatically, eventually leading it to becoming the first mode to appear for tori of aspect ratios $4 \leq AR \leq 8$. Experimental validation of this transition sequence for moderate aspect ratio tori is given by Sheard *et al.* [26].

Mode C is a true subharmonic mode, not found for a fixed circular cylinder but is allowed in the present case due to the breaking of symmetry by the torus curvature. Even for large aspect ratios, the loss of symmetry due to small curvature is still noticeable in the wake.

Direct numerical simulations using restricted spanwise arcs based on the preferred wavelengths determined from the Floquet instability analysis have been used to examine the saturated states. Figure 9 shows visualisations of these three modes for a torus of aspect ratio AR = 10. The spatio-temporal symmetry displayed by each mode can be observed from these plots.

2.3. Varying the shape to elongated cylinders

Ryan *et al.* [27] considered cylinders with elliptical leading edges and square trailing edges (see figure 3). The aerodynamic leading edge suppresses flow separation until the trailing edge. However, increasing elongation of the body results in a thickening boundary layer along the top and bottom sides of the body. The three-dimensional instability mode A is similar in critical wavelength and has the same spatio-temporal symmetry of mode A for a circular cylinder. As the cylinder is elongated, this mode becomes unstable at increasingly higher Reynolds number. Another mode that appears has some similarities to mode B for a circular cylinder, but is of a much longer wavelength (2.2*H*) and with a different perturbation field in the near wake. This mode, termed B′, possesses the same spatio-temporal symmetry as mode B – for example, the streamwise perturbation vorticity at any spanwise position maintains the same sign for each half cycle. Curiously, mode B′ becomes the most unstable mode for intermediate length cylinders; the difference between the Reynolds number at which onset of modes A and B′ occurs becomes greater with increasing aspect ratio.

By suppressing mode A in their computations, Karniadakis and Triantafyllou [15] found that mode B underwent period-doubling. Thus, the result that mode B′ occurs before mode A for aspect ratios
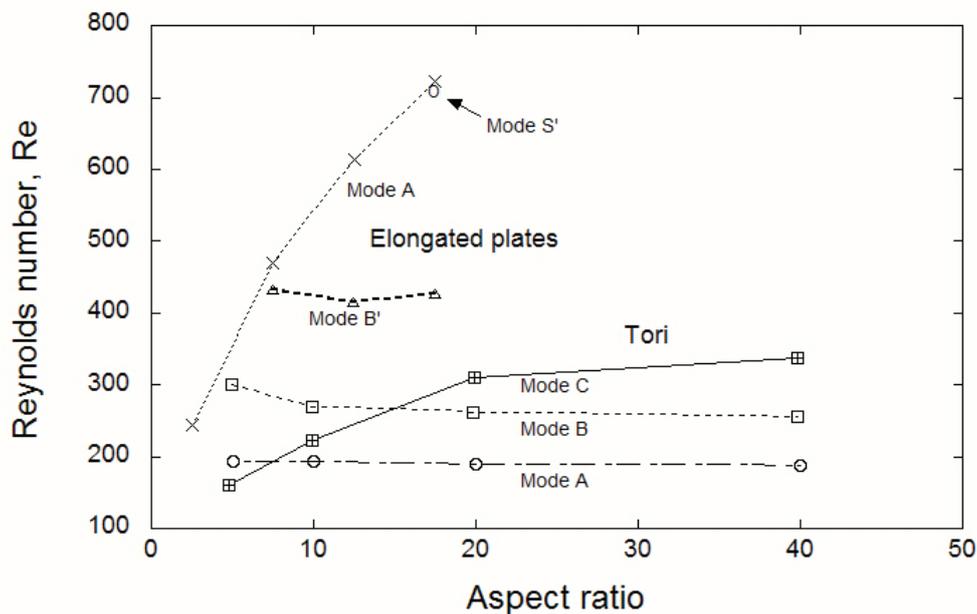
Figure 8. Critical Reynolds number for the onset of modes A, B and C for tori for aspect ratios $AR > 5$, and for modes A, B′ and S′ for elongated plates.
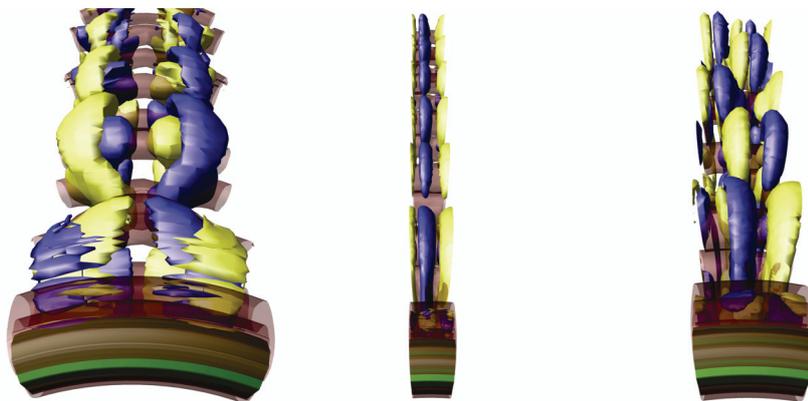

Figure 9. Perspective view of the three saturated instability modes for a large aspect ratio torus. In this case, AR = 10. The flow, from bottom to top, is visualized using isosurfaces of positive and negative streamwise vorticity, which reveals the spatio-temporal symmetry. Left to right, mode A (Re = 200), mode B (Re = 280) and mode C (Re = 235), respectively. Semi-transparent isosurfaces showing sections of the torus and the positions of the axi-symmetric rollers are also provided.

greater than approximately 7 may have implications for the route to turbulence for this bluff body distinct from that for the circular cylinder.

Figure 10 shows streamwise vorticity isosurfaces for Mode S′. This mode has also been observed in the wake of a square cylinder (Robichaux *et al.* [28]), where it was mistakenly believed to be a subharmonic mode. Ryan *et al.* [23] found that, for the elongated cylinder, the streamwise vorticity appeared to swap sign approximately, but not exactly, every full shedding cycle. The Floquet mode structure shown in figure 10 was obtained from a complex Floquet mode calculation, which allows for traveling modes as well as spatially stationary modes (see Blackburn and Lopez [29]). The real part of the Floquet multiplier only becomes greater than unity for large aspect ratio (AR, i.e., length to height ratio) cylinders, but eventually it too becomes more unstable than mode A (see figure 8 for an aspect ratio of 17.5).
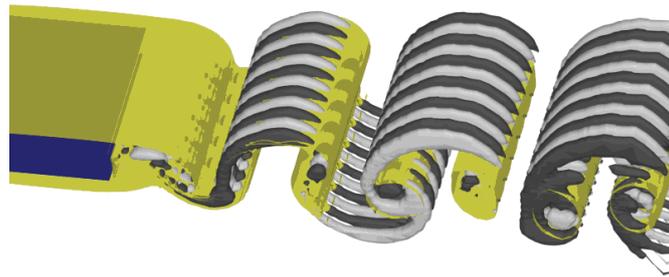
Figure 10. Stream-wise and span-wise vorticity components for mode S′ in the wake of an elongated cylinder with AR = 12.5.
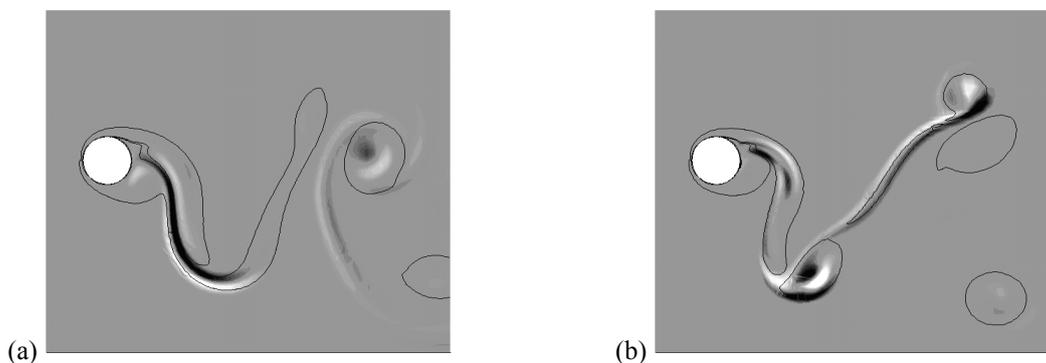

(a)   (b)

Figure 11. Spanwise perturbation vorticity for (a) mode SL, A*= 0.7, Re= 200 and λ = 1.5 and (b) mode SS, A*= 0.75, Re = 265 and λ = 0.80, of a transversely oscillating cylinder.

2.4. Varying the transverse oscillation of a circular cylinder
Finally, we consider the effect on the three-dimensional transition in the wake of a circular cylinder as the normalized transverse oscillation amplitude (A*) is varied at the Strouhal number for a fixed circular cylinder, 0.20. It was found that oscillation could delay the onset of three-dimensionality until the Reynolds number reached Re= 280. Also, while the two-dimensional wake retains the 2S configuration, the oscillation causes the order of the three-dimensional modes to change, with mode B becoming critical before mode A for A*> 0.3. With the transition of the base flow to the P + S wake mode at A*= 0.55, two new three-dimensional modes arise, modes SL and SS, both of which are subharmonic. For amplitudes where A*< 0.67, the P + S wake is inherently unstable to mode SL. This implies that a two-dimensional P + S wake mode cannot be physically realised over this amplitude range. For amplitudes up to A*< 0.72, mode SL becomes critical first. However, mode SL ceases to ever become critical for A*> 0.72, leaving mode SS as the leading three-dimensional mode (the spanwise perturbation vorticity for modes SL and SS is shown in figure 11).

3. Conclusions
In addition to the fixed circular cylinder case, a number of topological and body motion variations have been considered, with a view to determining if there is a universal nature of wake transitions behind bluff bodies. The four additional cases considered were: elliptical shaped bodies formed by the successive decrease in aspect ratio from circular cylinder to a flat normal plate: the varying of topology from locally that of a circular cylinder to a sphere through the decrease of aspect ratio of tori; the elongation of cylinders with elliptical leading edges and square trailing edges; and increasing the transverse amplitude of oscillation at fixed frequency of a circular cylinder.

Remarkably, in every case, there were at least significant regions of the parameter space where the transition sequence of three-dimensional modes was different from that for a fixed circular cylinder.

For example, for a torus and intermediate aspect ratios $4 \leq AR \leq 8$, the subharmonic mode C is the most unstable mode. On the other hand, for a normal flat plate, the most unstable mode is a long wavelength quasiperiodic mode. In the case of the elongated cylinders with a blunt trailing edge, an analog of mode B for the circular cylinder wake becomes unstable at an increasingly lower Reynolds number than mode A. Additionally, this mode B has a perturbation field structure that is very different in the near wake, and possesses a much longer preferred spanwise wavelength than mode B for a circular cylinder. For transversely oscillating circular cylinders, modes similar to the fixed case are found when the two-dimensional wake is in the 2S configuration. However, increasing the amplitude of oscillation sees the critical Reynolds number for mode A increase significantly, to the point where mode B becomes critical before mode A. For higher Reynolds numbers, the two-dimensional wake loses its spatio-temporal symmetry and takes on the P + S configuration. With the onset of this configuration, modes A, B and QP cease to exist and two new three-dimensional modes (SL and SS) arise.

The association of complex three-dimensional instability modes with generic physical instability mechanisms is beyond the scope of this article but has been considered by a number of authors (e.g., Leweke and Provansal [30]; Brede *et al.* [7]; Leweke and Williamson [31,32]; Thompson *et al.* [11,23]; Ryan *et al.* [27]; Julien *et al.* [21,22]). This will however be discussed at the Symposium.

Although there are still questions as to the effect that the different transition sequences and existence of different modes has on the route to turbulence or the final turbulent state, it is clear that the wake of the circular cylinder is far from universal for bluff bodies.

4. References

[1]   Roshko A 1955 On the wake and drag of bluff bodies *J. Aero. Sci.* **22** 124–32
[2]   Griffin O M 1981 Universal similarity in the wakes of stationary and vibrating bluff structures *ASME J. of Fluids Eng.* **103** No. 1 52–8
[3]   Williamson C H K 1988 The existence of two stages in the transition to three dimensionality of a cylinder wake *Phys. Fluids* **31** 3165–8
[4]   Williamson C H K 1996 Three-dimensional wake transition *J. Fluid Mech.* **328** 345–407.
[5]   Williamson C H K 1996 Vortex dynamics in the cylinder wake *Ann. Rev. Fluid Mech.* **28** 477–539
[6]   Wu J, Sheridan J, Welsh M C and Hourigan K 1996 Three-dimensional vortex structures in a cylinder wake *J. Fluid Mech.* **312** 201–22
[7]   Brede M, Eckelmann H and Rockwell D 1996 On secondary vortices in a cylinder wake *Phys. Fluids* **8** 2117–24
[8]   Bays-Muchmore B and Ahmed A 1993 On streamwise vortices in turbulent wakes of a cylinder *Phys. Fluids* A **5**(2) 387
[9]   Gerrard J H 1978 The wakes of cylindrical bluff bodies at low Reynolds numbers *Philos. Trans. R. Soc. London Ser.* A **288** 351–82
[10]   Thompson M C, Hourigan K and Sheridan J Three-dimensional instabilities in the cylinder wake *Proc. Int. Colloq. Jets, Wakes, Shear Layers* (*Melbourne, Australia, April 18-20 1994*) eds K Hourigan and I Shepherd (CSIRO)
[11]   Thompson M C, Hourigan K and Sheridan J 1996 Three-dimensional instabilities in the wake of a circular cylinder *Exp. Therm. Fluid Sc.* **12** 190–96
[12]   Barkley D, Henderson R D 1996 Three-dimensional Floquet stability analysis of the wake of a circular cylinder *J. Fluid Mech.* **322** 215–41
[13]   Henderson R 1997 Nonlinear dynamics and pattern formation in turbulent wake transition *J. Fluid Mech.* **352** 65–112
[14]   Mittal R and Balachandar S 1995 Generation of streamwise structures in bluff body wakes *Phys. Rev. Lett.* **75** 1300
[15]   Karniadakis G E and Triantafyllou G S 1992 Three-dimensional dynamics and transition to turbulence in the wake of bluff objects *J. Fluid Mech.* **238** 1–30

[16]   Sheard G J, Thompson M C and Hourigan K 2003 A coupled Landau model describing the Strouhal–Reynolds number profile of a three-dimensional circular cylinder wake *Phys. Fluids* (Letters) **15** (9) 68–71

[17]   Johnson S A, Thompson M C and Hourigan K 2004 Predicted low frequency structures in the wake of elliptical cylinders *Euro. J. Mech. B/Fluids* **23** (1) 229–39

[18]   Taneda S 1959 Downstream development of wakes behind cylinder *J. Phys. Soc. Jpn* **14** 843-50

[19]   Cimbala, J M, Nagib H M and Roshko A 1988 Large structures in the far wake of two-dimensional bluff bodies *J Fluid Mech.* **190** 265-98

[20]   Najjar F M and Balachandar S 1997 Low-frequency unsteadiness in the wake of a normal flat plate *J. Fluid Mech.* **370** 101–47

[21]   Julien S, Lasheras J and Chomaz J 2003 Three-dimensional instability and vorticity patterns in the wake of a flat plate *J. Fluid Mech.* **479** 155–89

[22]   Julien S, Ortiz S and Chomaz J-M 2004 Secondary instability mechanisms in the wake of a flat plate *Euro. J. Mech. B/Fluids* **23** (1) 157–65

[23]   Thompson M C, Leweke T and Williamson C H K 2001 The physical mechanism of transition in bluff body wakes *J. Fluids Struct.* **15** 607–16

[24]   Sheard G J, Thompson M C and Hourigan K 2003 From spheres to circular cylinders: the stability and flow structures of bluff ring wakes *J. Fluid Mech.* **492** 147–80

[25]   Sheard G J, Thompson M C and Hourigan K 2004 From spheres to circular cylinders: Non-axisymmetric transition in the flow past rings *J. Fluid Mech.* **506** 45–78

[26]   Sheard G J, Thompson M C, Hourigan K and Leweke T 2005 The evolution of a subharmonic mode in a vortex street *J. Fluid Mech.* **534** 23-38

[27]   Ryan K, Thompson M C and Hourigan K 2005 Three-dimensional transition in the wake of elongated bluff bodies *J. Fluid Mech.* **538** 1–29

[28]   Robichaux J, Balachandar S and Vanka S P 1999 Three-dimensional Floquet instability of the wake of square cylinder *Phys. Fluids* **11** 560–578

[29]   Blackburn H M and Lopez J M 2003 The onset of three-dimensional standing and modulated travelling waves in a periodically driven cavity flow *J. Fluid Mech.* **497**(1) 289-317

[30]   Leweke T and Provansal M 1995 The flow behind rings: Bluff body wakes without end effects *J. Fluid Mech.* **288** 265–310

[31]   Leweke T and Williamson C H K 1998 Cooperative elliptic instability of a vortex pair *J. Fluid Mech.* **360** 85–119

[32]   Leweke T and Williamson C H K 1998 Three-dimensional instabilities in wake transition E*uro. J. Mech. B/Fluids* **17** 571–86